PHYSICAL REVIEW A VOLUME 18, NUMBER 2 AUGUST 1978

Energy loss and straggling of protons and helium ions traversing some thin solid foils*

J. C. Eckardt
Comisión Nacional de Energía Atómica, Centro Atómico Bariloche, S.C. de Bariloche, R.N., Argentina
(Received 5 August 1976; revised manuscript received 23 May 1977)

Absolute measurements of stopping powers and energy straggling for hydrogen- and helium-ion beams in Ge, Se, Pd, Ag, Sb, and Bi in the energy range $20 \leq E \leq 260$ keV were performed by the method of determining the energy loss suffered by an ion beam which has traversed a thin film. The measured stopping powers fit reasonably well with those of other authors obtained at higher and lower ion energies. Agreement with theoretical predictions for energies >100 keV/amu is found to be better for hydrogen than it is for helium beams. The Z_2 dependence of the stopping power for hydrogen projectiles is discussed including measurements of other authors performed on other elements, and is found to agree in shape with that for helium for ion velocities $v > 2$ a.u., but there is evidence that it begins to differ with decreasing v. It is deduced from the present measurements that for hydrogen as well as helium ions the amplitude of oscillations of the Z_2 dependence increases with decreasing ion velocity, reaching a maximum at $v = 1.4$ a.u. The Lindhard-Scharff theory is found to be in satisfactory agreement with the measured energy straggling.

I. INTRODUCTION

The interest in the process of stopping of atomic projectiles in matter has increased lately with the development of the ion implantation technique for manufacturing semiconductor devices, and also with the increased use of backscattering of light ions from solid targets for the analysis of surface layers.

One parameter governing the stopping process is the stopping power dE/dR defined as the average energy loss suffered by an ion beam which has penetrated a distance dR in matter; or the stopping cross section defined as $S=(1/N)dE/dR$, where N is the number density of the target atoms. Another parameter is the energy straggling, defined as the standard deviation Ω of the energy distribution of an initially monoenergetic ion beam after traversing a distance dR through matter.

In the last years, several authors have presented measurements and theories of the oscillatory behavior of S, either as a function of Z_1, the projectile atomic number for a given target [1–11] or as a function of Z_2, the target atomic number, for a given projectile.[12–21] The most complete study of the structure of $S(Z_2)$ has been made by Chu *et al.*[16–19] for ^{4}He ions at energies above 400 keV. Chu[22] has also made theoretical calculations of the energy straggling Ω for protons and helium ions in the energy range $100 \leq E/m \leq 1000$ keV/amu and predicts an oscillatory behavior of $\Omega(Z_2)$ similar to that of $S(Z_2)$.

In order to investigate these phenomena for protons and for He^+ ions at lower energies where the existing information is very limited, we have performed measurements of energy loss and straggling of H^+- and He^+-ion beams in thin foils of Ge, Se, Pd, Ag, Sb, and Bi in the energy range $20 \leq E \leq 260$ keV.

II. EXPERIMENTAL

We used the most direct method for obtaining the stopping power dE/dR, i.e., the measurement of the energy loss ΔE suffered by an ion beam which has traversed a thin solid film of thickness ΔR. For the results to be reliable, ΔE should be only a small fraction of the energy E of the incoming beam. In the present work it was below 10% of E over most of the energy interval investigated, reaching in some cases about 20%–30% at the low-energy end.

The experimental procedure and equipment used for determining ΔE was described previously [20] The proton and $^4He^+$ beams where obtained by feeding the rf ion source of a Cockroft-Walton accelerator with a helium-hydrogen mixture, and for each energy used, each ion beam could be directed into the target chamber by adjusting the magnetic mass analyzer. The beam energy was measured with an electrostatic analyzer, and beam detection was performed by means of a scintillation counter. A prefixed fraction of the polarizing voltage of the electrostatic analyzer was swept with a voltage linearly increasing and decreasing in time (sweeping time = 6 sec). A signal proportional to the sweeping voltage was fed into the X input of an X-Y recorder, whose Y axis received the output of an integrator which in turn received from the scintillation counter a pulse rate proportional to the beam current. Since the current integrator of this dynamic recording system has a finite time constant, the spectra were deformed.[20] The curves obtained with the polarizing voltage of

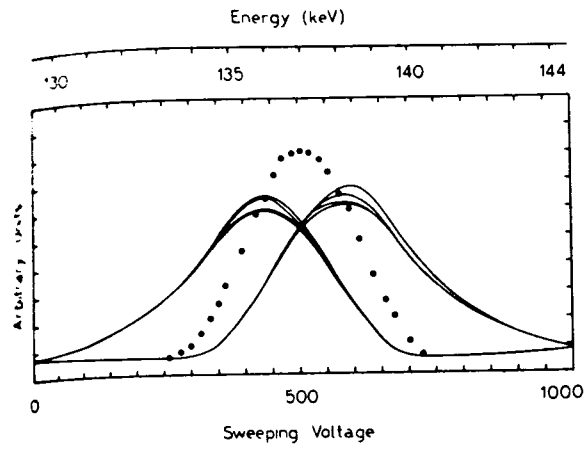

FIG. 1. Static spectrum taken point by point, and the corresponding dynamic response of the plotting device, of a ^{4}He-ion beam of an average energy of 137 keV, after traversing a 41.1-μg/cm^2 Bi foil, where it has lost 11.5 keV. Differences in subsequent dynamic plots are due to beam intensity fluctuations.

the electrostatic analyzer increasing linearly in time, had in all cases mirror symmetry with respect to those for decreasing voltage. This means that the real or static spectra were symmetric, and therefore the beam energy was given by the average of the plotted peak positions. A few spectra were also taken point by point. Figure 1 shows an example for such a static spectrum together with the corresponding dynamic response of the plotting device, for the case of a ^{4}He ion beam of an average energy of 137 keV, after traversing a Bi foil of 41.1-μg/cm^2 thickness, where it has lost 11.5 keV.

The real spectra corresponding to the measurements of the present work, could be approximated by a Gaussian function of energy as shown by straight lines obtained when plotting the static spectra on probability paper (see also Appendix of Ref. 20). This result is in accordance with the expectation that the energy profiles tend to be Gaussian when the energy lost in the foils is much greater than the maximum energy transfer by a projectile in a single collision with a target electron,[23] as it is the case in the present measurements.

To obtain the energy straggling, the standard deviation of the spectra had to be determined. As the shape of the real spectra was Gaussian, using the time constant of the dynamic device (it was measured to be $\tau = 0.70 \pm 0.02$ sec), it was possible to relate mathematically the distance between the plotted peaks, corresponding to increasing and decreasing sweeping voltages, with the standard deviation of the corresponding real spectrum. The mathematical formulation of this method is explained in detail in the Appendix. When, as in Fig. 1, the standard deviation could be obtained directly from the plot of the static spectrum on probability paper, it agreed within experimental error limits with that obtained from the distance between peaks of the dynamic plot.

In practice the incoming beam was not monoenergetic, but had also a Gaussian-like energy distribution. Therefore, to determine the energy straggling the standard deviation of the beam energy profile was also measured in each case (ranging typically between 50 and 900 eV at 25 and 260 keV, respectively) and substracted geometrically from that corresponding to the beam after traversing the foil.

The foils were prepared employing basically the method developed by Meckbach[24] and Valenzuela and Eckardt[25] which consists in the vacuum deposition of the foil onto a plastic substrate which is subsequently dissolved. A vacuum in the evaporator of about 2×10^{-7} Torr was achieved using titanium sublimation and ionic pumping which provided an oil-free environment. The thickness Δx in μg/cm^2, was measured in the evaporator, by weighing the deposit on a piece of plastic substrate of known area, suspended from a Cahn-RG electric microbalance. A further control of film growth was made with the aid of a quartz-crystal film thickness monitor TOYO COM type TVF-1.

To ascertain the amount of contamination of the foil surface by oxidation, after evaporation was completed the pressure in the system was raised to about 10^{-5} Torr by admitting atmospheric air through a needle valve. After at least 10 min exposure, no mass increase due to oxidation of the deposit was observed, within experimental uncertainties (0.5%). This insures that the initial fast oxidation of both surfaces of the foils by exposure to air[26] influences the stopping power measurements by less than 2% in each case.

For each element, between 11 and 24 foils were used, except in the case of Sb, where only three were used. The thicknesses of most of these foils ranged between 21 and 44 μg/cm^2, two of the Pd foils were of 17.7 μg/cm^2 and one Ag foil, used only for protons, was 11.3 μg/cm^2 thick. The diameter of the foils was 2 mm.

Sample foils were observed with an electron microscope. They were found to be of uniform structure and no pinholes were apparent. Also moving the foil across the ion beam (of <1 mm in diameter) did not affect the measured energy loss nor the shape of spectra, within experimental uncertainties.

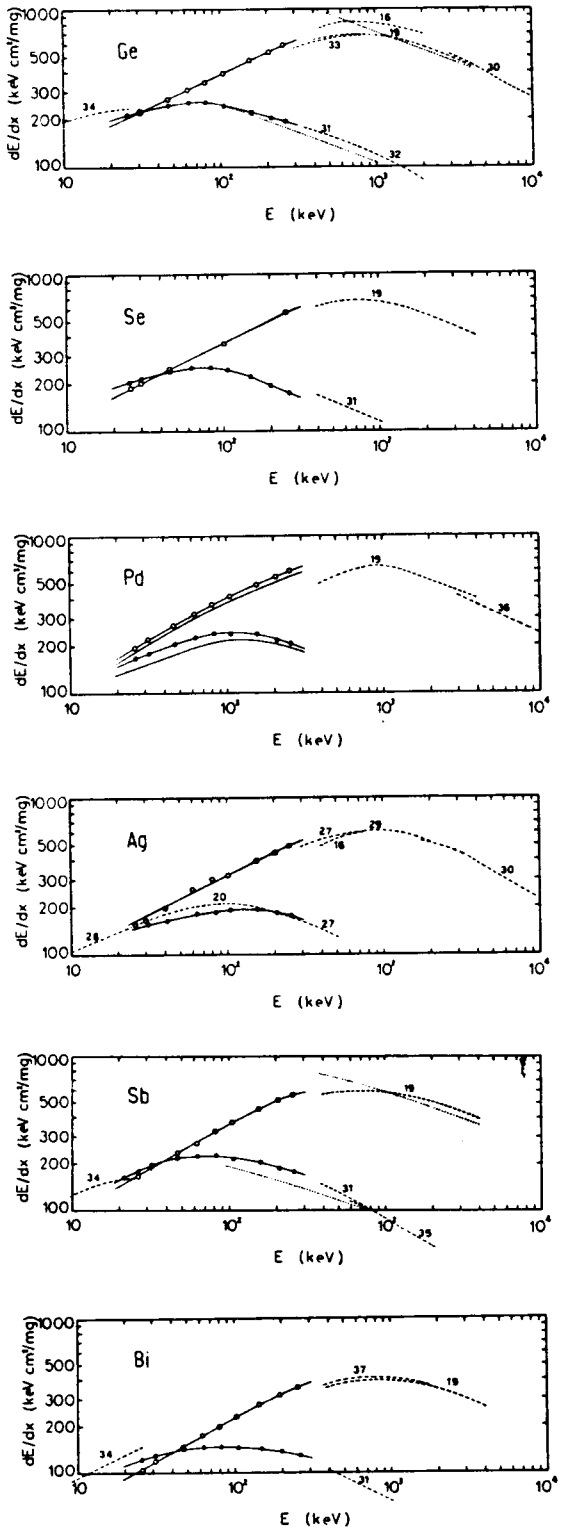

FIG. 2. Stopping powers for proton and $^4He^+$ beams as a function of energy. —·—, protons; —∘—, $^4He^+$; -----, other authors[16,19,20,27-37]; the numbers on the figure identify the reference. ....., theory.[19] ———, corrected values for possible content of absorbed hydrogen in Pd.[39]

III. RESULTS

A. Energy loss

The experimental results of the stopping powers of the studied materials for hydrogen and helium ions are shown in Fig. 2, together with experimental and semiempirical data from other authors[16,19,20,27-37] for comparison. Tables I and II present the values obtained by graphical interpolation between data points.

The uncertainties of the measured stopping powers calculated as the percentage mean deviation over all foils used[38] are 6%, 2%, 7%, 5%, 7%, and 5%, for Ge, Se, Pd, Ag, Sb, and Bi respectively, and are mainly due to uncertainties in the determination of foil thicknesses.

Pd may contain absorbed hydrogen up to the proportion of Pd_4H_3.[39] Figure 2 also shows corrected values for Pd using Bragg's rule of additivity of stopping cross sections. It can be seen that the possible content of hydrogen may affect the measurements only up to 10%.

B. Energy straggling

Because of its statistical nature, the energy straggling due to subsequent layers of the foil is added geometrically, i.e., the straggling is proportional to the square root of foil thickness. The present results, normalized by dividing them by the square root of Δx are shown in Fig. 3. Tables I and II also list the $\Omega/(\Delta x)^{1/2}$ values for the different elements for protons and $^4He^+$ obtained by graphical interpolation between data points. These values are affected by a statistical error of about ±10%.

The principal source of systematic error in the determination of the energy straggling of ion beams in solid foils is the possible microscopic roughness of the foils. The energy spread produced by this possible foil roughness is directly proportional to the stopping power. Since the curved behavior of the stopping power for protons as a function of energy in logarithmic scale (Fig. 2) does not appear in the straggling measurements for protons (Fig. 3), it can be assumed that this contribution to the measured energy straggling is small.

IV. DISCUSSION AND CONCLUSION

A. Energy loss

1. Comparison with theory

a. Energy dependence. Ziegler and Chu[19] have calculated theoretical stopping cross sections in the Lindhard-Winther[40] formalism with Hartree-Fock-Slater atomic wave functions for isolated target atoms, for ^4He ions in all elements in the

TABLE I. Stopping powers and energy straggling for hydrogen ions obtained by graphical interpolation between data points. E_0 in keV; dE/dx in keV/(mg/cm^2); $\Omega/(\Delta x)^{1/2}$ in eV $(\mu g/cm^2)^{-1/2}$.

	Germanium		Selenium		Palladium			Silver		Antimony		Bismuth	
$^1H^+$ E_0	$\frac{dE}{dx}$	$\Omega/(\Delta x)^{1/2}$	$\frac{dE}{dx}$	$\Omega/(\Delta x)^{1/2}$	$\frac{dE}{dE}$	$\frac{dE}{dx}$[a]	$\Omega/(\Delta x)^{1/2}$	$\frac{dE}{dx}$	$\Omega/(\Delta x)^{1/2}$	$\frac{dE}{dx}$	$\Omega/(\Delta x)^{1/2}$	$\frac{dE}{dx}$	$\Omega/(\Delta x)^{1/2}$
20	200	77	191	41	148	132	66	138	85	155	90	112	55
30	223	88	217	48	175	152	78	155	100	188	102	129	64
40	240	97	232	54	195	168	88	166	113	208	110	138	71
60	257	110	252	63	223	194	106	180	133	222	124	147	82
80	259	121	255	71	238	211	120	189	150	223	134	148	92
100	251	130	250	77	245	218	132	193	165	221	143	147	100
150	227	148	221	91	240	218	158	195	195	206	160	142	116
200	211	163	197	102	223	208	179	188	219	192	174	137	129
300	187	185	166	119	195	183	213	169	259	171	195	126	150

[a]Values corrected for possible content of absorbed hydrogen.[39]

energy region 400–4000 keV. Their expression of the stopping cross section is proportional to Z_1^2, the square of the projectile atomic number, irrespective of charge states $<Z_1$ in the beam. This allows one to transform their theoretical stopping cross-section data for ^{4}He projectiles into those for ^{1}H projectiles of equal velocity i.e., energies of 100–1000 keV, by simply dividing by 4, the square of the atomic number of He. The theoretical data for He and those obtained in this way for hydrogen projectiles, are represented in Fig. 2 for Ge and Sb. It may be observed that while the theory fails for 400-keV ^{4}He projectiles,[41] it still holds rather well for 100-keV protons.

b. Z_2 dependence. We compare in Fig. 4 the present results for protons, together with data of other authors,[2,3,15,20,27,42-45] as a function of Z_2 for ion energies of 100, 200, and 300 keV with the theoretical values given in Ref. 19 for ^{4}He, reduced for protons as described above. It is seen that the oscillatory behavior of this theory agrees qualitatively with the experimental data presented in this figure, as it does for helium projectiles at energies greater than 400 keV.[19]

2. *Experimental Z_2 dependence for protons compared with that for ^{4}He ions*

The present measurements, performed with hydrogen and helium ions in the same foils under identical experimental conditions make it possible to compare $S(Z_2)$ for both projectiles directly by taking the ratio S_{He}/S_H at equal velocities. As only data for a few elements are available it was not meaningful to represent this ratio as a function of Z_2. Instead, we show in Fig. 5 the average ratios S_{He}/S_H which result from the measurements of stopping powers in the elements used in the present work. The error bars shown in Fig. 5, given by the mean deviations of these ratios, are a measure of the fluctuations of S_{He}/S_H obtained in targets of different Z_2. We observe that the mean

TABLE II. Stopping powers and energy straggling for helium ions obtained by graphical interpolation between data points. E_0 in keV; dE/dx in keV/(mg/cm^2); $\Omega/(\Delta x)^{1/2}$ in eV $(\mu g/cm^2)^{-1/2}$.

	Germanium		Selenium		Palladium			Silver		Antimony		Bismuth	
$^4He^+$ E_0	$\frac{dE}{dx}$	$\Omega/(\Delta x)^{1/2}$	$\frac{dE}{dx}$	$\Omega/(\Delta x)^{1/2}$	$\frac{dE}{dE}$	$\frac{dE}{dx}$[a]	$\Omega/(\Delta x)^{1/2}$	$\frac{dE}{dx}$	$\Omega/(\Delta x)^{1/2}$	$\frac{dE}{dx}$	$\Omega/(\Delta x)^{1/2}$	$\frac{dE}{dx}$	$\Omega(\Delta x)^{1/2}$
20	183	72	164	39	168	155	68	145	112	142	87	92	54
30	221	88	201	49	213	200	84	177	131	180	107	115	69
40	253	100	232	58	252	236	97	204	147	213	123	135	82
60	306	120	283	74	315	295	118	251	171	270	152	170	104
80	350	138	327	88	367	343	136	289	191	317	176	200	123
100	390	153	365	100	407	380	151	323	208	360	198	227	140
150	470	183	445	128	488	451	185	393	243	444	243	283	176
200	537	210	515	151	548	505	212	450	273	510	282	324	208
300	640	254	618	191	640	585	260	538	318	578	346	385	263

[a]Values corrected for possible content of absorbed hydrogen.[39]

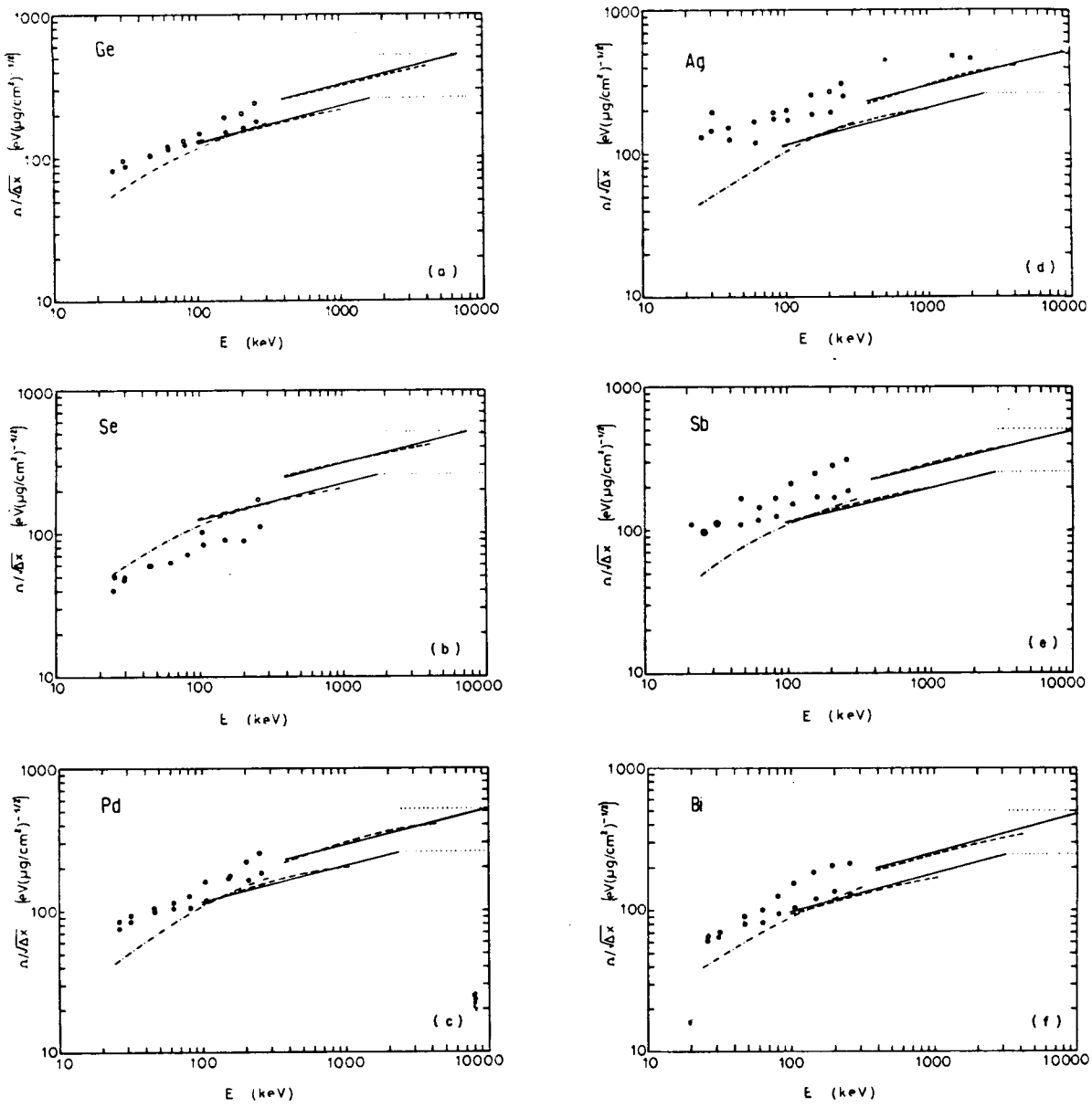

FIG. 3. Energy straggling as a function of energy. ● and ○, data points of the present work for protons and $^4He^+$, respectively. Big points for Sb indicate proton and $^4He^+$ data together. ■, experimental data of Hoffman and Powers[55] for α particles in Ag. ....., Bohr[54] theory for high energies; ———, Lindhard and Scharff[62] theory; – – – –, calculated data by Chu.[22] Upper and lower curves correspond to ^4He ions and protons, respectively. -·-·-·-·-, estimates for protons using the Lindhard and Scharff[62] formula, but including experimental dE/dx data.

fluctuations obtained in this manner are not important compared to the remarkable structure in the stopping cross sections for He and H beams as a function of Z_2, which has been cancelled out in their ratio, and also that excellent agreement exists with the ratios obtained by Meckbach and Allison in Cd foils.[46] However, it is also seen that the mean fluctuations increase at the lower ion velocities. While at $v = 1.8$ a.u. the mean deviation is only 4.3% it increases up to 11.5% at $v = 0.9$ a.u. This indicates that the difference between the Z_2 dependence of the stopping cross sections of He and H beams is greater at these low velocities where the contribution of charge exchange to the stopping process may be significant, as suggested by the work of Allison *et al.*[47] on partial stopping powers in gaseous targets.

At ion velocities ≥ 2 a.u. a direct comparison of the $S(Z_2)$ dependence for H and He projectiles is possible by using the experimental information

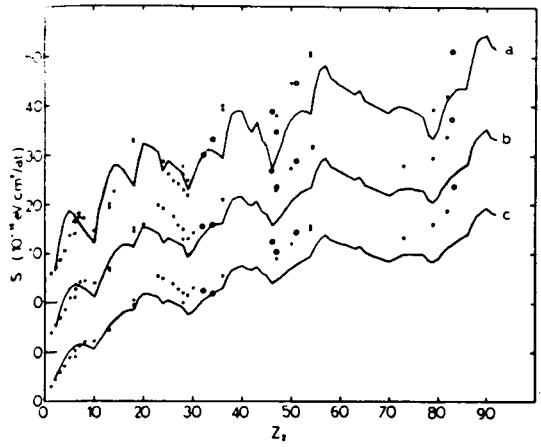

FIG. 4. $S(Z_2)$ for protons, (a) 100 keV; (b) 200 keV; (c) 300 keV. O, present results; ●, compiled data[2,3,15,20,27,42-45]; ———, theory[19] adapted for protons.

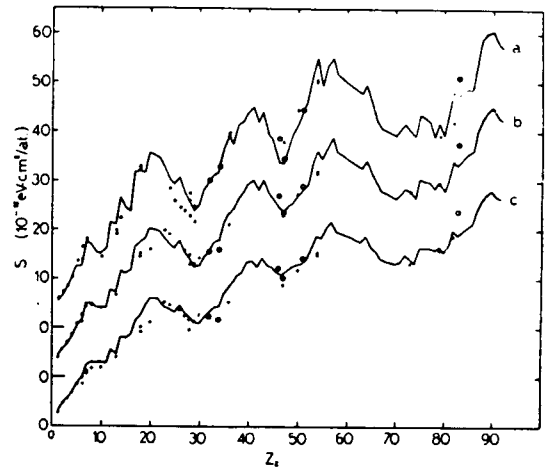

FIG. 6. $S(Z_2)$ for protons: (a) 100 keV; (b) 200 keV; (c) 300 keV. O, present results; ●, compiled data[2,3,15,20,27,42-45]; ———, semiempirical data for ^{4}He projectiles[19] of 400, 800, and 1200 keV normalized to protons.

from other authors[2,3,15,20,27,42-45] as seen in Fig. 4 and dividing the semiempirical stopping cross sections for ^{4}He of Ziegler and Chu by the stopping power ratios S_{He}/S_H averaged over all available data. Figure 6 shows this comparison which strikingly confirms the agreement of $S(Z_2)$ for He and H ions. This is in accordance with a previous publication,[48] where we have suggested that for ion velocities $v > 2$ a.u. the Z_2 dependence is the same for different ions of equal velocity except for a factor which depends only on v and on Z_1, the projectile atomic number, but not on Z_2.

Since for low velocities no data of S are available for elements situated at a maximum of the Z_2 oscillations, it is not possible to obtain a direct measure of the amplitude of these oscillations. Notwithstanding that, it is possible to obtain a value related directly to the behavior of the amplitude for different ion velocities by comparing the S of one element situated in a minimum with that of another situated away from it. Here Sb and Ag have been chosen for this purpose. Figure 7 shows the quotients $S(\mathrm{Sb})/S(\mathrm{Ag})$ for protons and ^{4}He$^+$ as a function of the ion velocity. It can be observed that this magnitude, related to the amplitude of the oscillations, increases as v decreases, reaching a maximum at $v = 1.4$ a.u. for protons as well as for ^{4}He$^+$. To extend the curve corresponding to ^{4}He$^+$ up to $v = 3.46$ a.u., the data of Ref. 27 for Ag and of Ref. 19 for Sb were used.

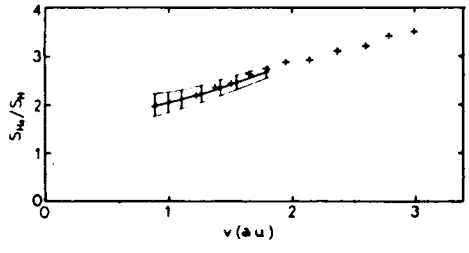

FIG. 5. Ratios S_{He}/S_H averaged over Ge, Se, Pd, Ag, Sb, and Bi, and their mean deviation, as a function of ion velocity + data corresponding to Cd foils.[46]

B. Energy straggling

Figure 3 shows our results for the energy straggling as a function of ion energy for protons and helium ions. In this energy range, the straggling can be approximated by

$$\Omega/(NdR)^{1/2} = KE^P, \tag{1}$$

where E is the ion energy and P has in the average a value of 0.37 for protons and 0.5 for helium ions.

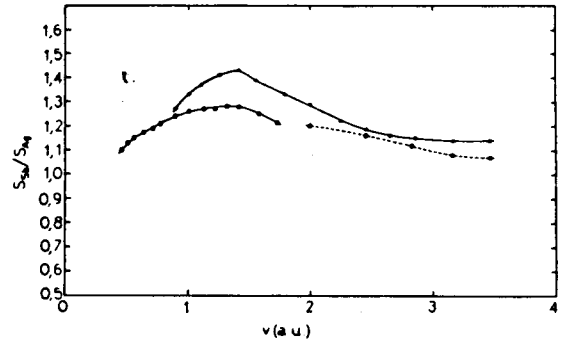

FIG. 7. Ratios S_{Sb}/S_{Ag} (a magnitude related with the amplitude of the Z_2 oscillations) as a function of ion velocity. ●, protons; O, helium ions; ———, present results; --------, data from Ref. 27 for S_{Ag} and Ref. 19 for S_{Sb}.

This approximately linear velocity dependence for $^4He^+$ is in fair agreement with experimental data of Hvelplund[49] for He ions in gas targets, and with his formula obtained from

$$\frac{\Omega^2}{NdR} = \int 2\pi b \epsilon^2(b)\, db\,, \tag{2}$$

where $\epsilon(b)$ is the energy loss as a function of the impact parameter b as derived by Firsov[50] for many-electron atoms. The integration is performed from $b=0$ to $b=\infty$. However, Firsov's theory considers straight line trajectories and is not valid, therefore, for small impact parameters. On the other hand, Lindhard's theory[51] of stopping in a degenerate electron gas gives also $\Omega \propto v$ in the limit of low velocities.

By analogy with the results for an electron gas, Lindhard and Scharff[52] have proposed

$$\frac{\Omega^2}{NdR} \cong \frac{1}{2}\, mv^2 \frac{dE}{NdR}\,, \tag{3}$$

valid for $Z_1^2 < (v/v_0)^2 < 3Z_2$. Here m is the electron mass and v_0 the Bohr velocity. Equation (3) is obtained from Eq. (17) of Ref. 52 after rearrangement of terms. We have calculated

$$\Omega/(\Delta x)^{1/2} = \Omega/(AN\Delta R/N_a)^{1/2}\,, \tag{4}$$

(A being the target atomic mass, and N_a Avagadro's number) from Eq. (3), using our measured values of stopping and also using the Lindhard and Scharff approximation[52]

$$\frac{dE}{NdR} = \frac{4\pi Z_1^2 e^4 Z_2}{mv^2}\,(1.36\, x^{1/2} - 0.016\, x^{3/2})\,, \tag{5}$$

with $x = v^2/v_0^2 Z_2$, valid in the region where the stopping power is inversely proportional to v. The results of these calculations are included in Fig. 3.

In the derivation of Eq. (5) Lindhard and Scharff applied the theory for a uniform electron gas to the case of atoms, where the electron density varies quite rapidly in space. This is a dubious procedure as recognized by these workers but which, nevertheless, by inclusion of an empirical constant to account for the binding forces of the electrons in the atom, has been shown[19,53] to reproduce stopping power data successfully in the region of high velocities ($v > 2Z_1 v_0$).

Recently, Chu[22] has done calculations with this theory, but using Hartree-Fock-Slater charge densities for isolated atoms and found an oscillatory behavior of Ω as a function of Z_2. His results are also shown in Fig. 3 where it can be seen that, for the particular targets used in this work, they do not differ much from the simpler Lindhard-Scharff theory.

Finally, we have shown in Fig. 3 the classical result of Bohr[54] for high velocities,

$$\Omega_B^2/NdR = 4\pi Z_1^2 Z_2 e^4\,, \tag{6}$$

and the recent experimental data of Hoffman and Powers[55] for He ions in Ag, which agree well with the extrapolation of our results to higher energies.

The theories cited above treat the energy straggling due to collisions with electrons, i.e., due to inelastic stopping processes. As shown by Hvelplund,[49] the contribution of elastic encounters with target atoms is small in the present velocity range when the energy loss is measured over a small angular range (1.9×10^{-5} str in our case) around the forward direction.

ACKNOWLEDGMENTS

I am grateful to my colleagues for their help. Special thanks are due to W. Meckbach and to R. A. Baragiola for stimulating discussions and helpful suggestions.

APPENDIX

Since the energy spectra were taken with a dynamic recording system which has a time constant τ, the spectra obtained were deformed (see Appendix of Ref. 20). The differential equation governing the response of such a system is given by

$$\tau \frac{du(t)}{dt} + u(t) = u_s(t)\,; \tag{7}$$

by putting $\tau = 0$ it is seen that $u_s(t)$ represents the "static profile" one would get using a static system.

In the present experiment, $u_s(t)$ could be approximated by a Gaussian[20]: $u_s(t) = Ae^{-\alpha t^2}$ (putting the origin at the symmetry axis); then the solution to Eq. (7) is given by

$$u(t) = \frac{A}{2\tau}\left(\frac{\pi}{\alpha}\right)^{1/2} e^{1/4\alpha\tau^2} e^{-t/\tau} \cdot \left[1 + \operatorname{erf}\left(\alpha^{1/2} t - \frac{1}{2\alpha^{1/2}\tau}\right)\right]\,, \tag{8}$$

from the measured curves the value t_0 is obtained, which is one half the distance between the peaks of the plots corresponding to increasing and decreasing sweeping voltage, i.e., the abscissa for which $u(t)$ has its maximum. At this point

$$\frac{du(t_0)}{dt} = 0$$

and from Eq. (7)

$$u(t_0) = u_s(t_0)\,,$$

i.e.,

$$\frac{1}{2\tau}\left(\frac{\pi}{\alpha}\right)^{1/2} e^{1/4\alpha\tau^2} e^{-t_0/\tau} \times\left[1+\operatorname{erf}\left(\alpha^{1/2}t_0-\frac{1}{2\alpha^{1/2}\tau}\right)\right]=e^{-\alpha t_0}\,. \quad (9)$$

since t_0 is known, α is then obtained by numerical calculation and with it the standard deviation ω of the Gaussian given by

$$\omega=(1/2\alpha)^{1/2}\,. \quad (10)$$

It is significant to note from Eq. (9) that α is independent of the height A of the spectra.

•This work has been supported partially by the Organization of American States, Multinational Program in Physics.

[1]P. Hvelplund and B. Fastrup, Phys. Rev. 165, 408 (1968).

[2]J. H. Ormrod, J. R. MacDonald, and H. E. Duckworth, Can. J. Phys. 43, 275 (1965).

[3]J. R. MacDonald, J. H. Ormrod, and H. E. Duckworth, Z. Naturforsch. A 21, 130 (1966).

[4]B. E. Baklitsky, E. S. Parilis, and V. H. Ferleger, Radiat. Eff. 19, 155 (1973).

[5]C. P. Bhalla and J. N. Bradford, Phys. Lett. A 27, 318 (1968).

[6]I. M. Cheshire, G. Dearnaley, and J. M. Poate, Proc. R. Soc. Lond. A 311, 47 (1969).

[7]I. M. Cheshire and J. M. Poate, *Atomic Collision Phenomena in Solids* (North-Holland, Amsterdam, 1970), p. 351.

[8]A. H. El. Hoshy and J. F. Gibbons, Phys. Rev. 173, 454 (1968).

[9]D. E. Harrison, Appl. Phys. Lett. 13, 277 (1968).

[10]V. S. Kessellman, Zh. Tekh. Fiz. 42, 1161 (1972) [Sov. Phys.-Tech. Phys. 17, 923 (1972)].

[11]K. B. Winterbon, Can. J. Phys. 46, 2429 (1968).

[12]M. Bader, R. E. Pixley, F. S. Mozer, and W. Whaling, Phys. Rev. 103, 32 (1956).

[13]F. Bernhard, U. Müller-Jahreis, G. Rockstroh, and S. Schwabe, Phys. Status Solidi 35, 285 (1969); P. Apel, U. Müller-Jahreis, G. Rockstroh, and S. Schwabe, Phys. Status Solidi A 3, 173 (1970).

[14]W. Pietsch, U. Hauser, and W. Neuwirth, Nucl. Instrum. Methods 132, 79 (1976).

[15]W. White and R. M. Mueller, Phys. Rev. 187, 499 (1969).

[16]W. K. Chu and D. Powers, Phys. Rev. 187, 478 (1969).

[17]C. C. Rousseau, W. K. Chu, and D. Powers, Phys. Rev. A 4, 1066 (1971).

[18]W. K. Chu and D. Powers, Phys. Lett. A 38, 267 (1972).

[19]J. F. Ziegler and W. K. Chu, Atomic and Nuclear Data Tables 13, 463 (1974).

[20]A. Valenzuela, W. Meckbach, A. J. Kestelman, and J. C. Eckardt, Phys. Rev. B 6, 95 (1972).

[21]D. J. Land and J. G. Brennan, Nucl. Instrum. Methods 132, 89 (1976).

[22]W. K. Chu, Phys. Rev. A 13, 2057 (1976).

[23]U. Fano, Ann. Rev. Nucl. Sci. 13, 1 (1963).

[24]W. Meckbach, Rev. Sci. Instrum. 34, 188 (1963).

[25]A. Valenzuela and J. C. Eckardt, Rev. Sci. Instrum. 42, 127 (1971).

[26]For oxidation of clean surfaces at room temperature, the reader is referred, for example, to N. Cabrera and N. F. Mott, Rep. Prog. Phys. 12, 163 (1949); or to A. A. Frantsuzow and N. J. Makrushin, Bull. Acad. Sci. USSR Phys. Ser. 38, 187 (1974).

[27]D. J. Porat and K. Ramavataram, Proc. Phys. Soc. Lond. 78, 1135 (1961).

[28]K. Morita, H. Akimune, and I. Suita, J. Phys. Soc. Jpn. 25, 1525 (1968).

[29]E. Leminen and A. Fontell, Radiat. Eff. 22, 39 (1974).

[30]D. Ward, R. K. Graham, and J. S. Geiger, Can. J. Phys. 50, 2302 (1972).

[31]D. W. Green, J. W. Cooper, and J. C. Harris, Phys. Rev. 98, 466 (1955).

[32]S. Gorodetzky, A. Pape, E. L. Cooperman, A. Chevallier, J. C. Sens, and R. Armbruster, Nucl. Instrum. Methods 70, 11 (1969).

[33]W. K. Lin, H. G. Olson, and D. Powers, J. Appl. Phys. 44, 3631 (1973).

[34]E. P. Arkhipov and Yu. V. Gott, Zh. Eksp. Teor. Fiz. 56, 7746 (1969) [Sov. Phys. JETP 29, 615 (1969)].

[35]E. Leminen and A. Antilla, Ann. Acad. Sci. Fenn. A 6, 370 (1971).

[36]S. Rosenblum, Ann. Phys. (Paris) 10, 408 (1928).

[37]J. A. Borders, Radiat. Eff. 21, 165 (1974).

[38]J. C. Eckardt, Ph.D. thesis, Inst. de Física "Dr. José A. Balseiro," Bariloche, Argentina (1976).

[39]N. V. Sidgwick, *Chemical Elements and Their Compounds* (Clarendon Press, Oxford, 1950), Vol. II, p. 1554.

[40]J. Lindhard and A. Winther, Mat. Fys. Medd. 34, No. 4 (1964).

[41]W. K. Chu, V. L. Moruzzi, and J. F. Ziegler, J. Appl. Phys. 46, 2817 (1975).

[42]W. Whaling, *Handbuch der Physik, Vol. XXXIV* (Springer-Verlag, Berlin, 1958), p. 193.

[43]C. A. Sautter and E. J. Zimmermann, Phys. Rev. 140, 490 (1965).

[44]R. L. Wolke, W. N. Bishop, E. Eichler, N. R. Jonson, and G. D. O'Kelly, Phys. Rev. 129, 2591 (1963).

[45]C. Foster, W. H. Kool, W. F. Van der Weg, and H. E. Rossendaal, Radiat. Eff. 16, 139 (1972).

[46]W. Meckbach and S. K. Allison, Phys. Rev. 132, 294 (1963).

[47]J. Cuevas, M. García-Muñoz, P. Torres, and S. K. Allison, Phys. Rev. 135, A335 (1964).

[48]J. C. Eckardt, W. Meckbach, and R. A. Baragiola, Radiat. Eff. 27, 179 (1976).

[49]P. Hvelplund, Mat. Fys. Medd. 38, No. 4 (1971).

[50]O. B. Firsov, Zh. Eksp. Teor. Fiz. 36, 1517 (1959) [Sov. Phys. JETP 9, 1076 (1959)].

[51]J. Lindhard, Mat. Fys. Medd. 28, No. 8 (1954).

[52]J. Lindhard and M. Scharff, Mat. Fys. Medd. 27, No. 15 (1953).

[53]E. Bonderup and P. Hvelplund, Phys. Rev. A 4, 562 (1971).

[54]N. Bohr, Mat. Fys. Medd. 18, No. 8 (1948).

[55]G. E. Hoffman and D. Powers, Phys. Rev. A 13, 2042 (1976).